Flexible and printable dielectric polymer composite with tunable permittivity and thermal stability

Journal:	*ChemComm*
Manuscript ID	CC-COM-11-2019-008648.R1
Article Type:	Communication

COMMUNICATION

Flexible and printable dielectric polymer composite with tunable permittivity and thermal stability

Received 00th January 20xx,
Accepted 00th January 20xx

DOI: 10.1039/x0xx00000x

Feng Hu,[a] Lu An,[a] Aditya Tushar Chivate,[b] Zipeng Guo,[b] Saurabh Vishwas Khuje,[b] Yulong Huang,[a] Yong Hu,[a] Jason Armstrong,[a] Chi Zhou,[b] Shenqiang Ren[a,c,d,*]

Lightweight and printable polymer dielectrics are ubiquitous in flexible hybrid electronics, exhibiting high breakdown strength and mechanical reliability. However, its advanced electronic applications are limited due to its relative low permittivity, compared to its ceramic counterparts. Here we report flexible all organic percolative nanocomposites that contain in-situ grown conductive polymer networks and dielectric polymer matrix, in which their dielectric properties can be designed and guided from the percolation theory. High dielectric constant of all organic percolative nanocomposite is shown over a broad frequency range under intensive bending cycles, while its thermal stability is attributed to thermal conductive 2D montmorillonite nanosheets. The printable polymer composites with high dielectric performance and thermal stability would find broader interests in flexible hybrid electronics and radio frequency devices.

Dielectric materials with high dielectric constant and low loss are of great significance towards a wide range of applications in modern electronics and electrical power systems such as antenna electronics, hybrid electric vehicles and switched mode power supplies.[1-3] Compared with inorganic dielectric ceramics, lightweight polymers exhibit a high dielectric breakdown strength and hybrid manufacturing potential.[4-5] Dielectric polymers, such as poly(vinylidene fluoride) (PVDF), biaxially oriented polypropylene (BOPP), poly(ethylene terephthalate) (PET), polycarbonate (PC) have been attracting wide attention.[6] Among them, PVDF-based polymers have been extensively studied due to its high breakdown strength while its energy density is limited by its relatively lower permittivity.[7-9] Percolation theory for enhancement of dielectric constant has been applied into metal-polymer composites by using metal nanoparticles as fillers and epoxy as polymer matrix.[10-13] The hybrid composites containing dielectric ceramic or conductive metal fillers can therefore achieve high dielectric constant and high electric breakdown strength corresponding to the functions of additives and polymer matrix, respectively.[14,15] However, the ceramic or metal nanoparticle doped polymer composites can deteriorate its mechanical quality due to the aggregation of nanoparticles and dissimilar interfacial interactions. The incompatible inorganic-organic interface requires improvement, especially at a relatively high concentration of conducting additives.[16-17] In addition, polymer dielectrics often function at a relatively low operating temperatures.[18]

Here, we report an all organic printable dielectric polymer composite, where polyaniline (PANi) doped with protonic acid (HPANi) is applied as the conductive filler within the poly(vinylidene fluoride-trifluoroethylene) (PVDF-TrFE) copolymer matrix to enable the conductor-insulator dielectric composite. Under the HPANi percolation network strategy, a small fraction of HPANi conductive networks can bring a dramatic increase of dielectric constant while preserving the mechanical flexibility of the polymer.[13, 19-21] The percolative HPANi chain within the dielectric polymer matrix enables the bulk heterojunction structure to maintain the polymeric features of being lightweight with excellent mechanical elasticity.[13, 22] Meanwhile, PVDF-based dielectric polymers exhibit large spontaneous polarization and high dielectric constants because of the presence of highly electronegative fluorine on the polymer chains and the spontaneous alignment of C-F dipoles in the crystalline phases.[23, 24] We demonstrate a high thermal stability of the dielectric composite by templating 2D montmorillonite (MTM) nanosheet with the HPANi distributed into the PVDF-TrFE polymer matrix, enabling a high dielectric constant with improved thermal stability. HPANi functionalization of 2D MTM is achieved by in-situ polymerization of aniline in aqueous HCl solution in the presence of liquid-exfoliated 2D MTM nanosheets and ammonium persulfate. By introducing the HPANi-MTM heterostructures into the PVDF-TrFE polymer matrix, the

---

[a] *Department of Mechanical and Aerospace Engineering, University at Buffalo, The State University of New York, Buffalo, NY 14260*
[b] *Department of Industrial and Systems Engineering, University at Buffalo, The State University of New York, Buffalo, NY 14260*
[c] *Research and Education in Energy, Environment & Water Institute, University at Buffalo, The State University of New York, Buffalo, NY 14260*
[d] *Department of Chemistry, University at Buffalo, The State University of New York, Buffalo, NY 14260*
* Corresponding author: E-mail: shenren@buffalo.edu

Electronic Supplementary Information (ESI) available: [details of any supplementary information available should be included here]. See DOI: 10.1039/x0xx00000x

composite sheet containing 1 wt% of HPANi-MTM shows a 69.4% enhancement of the dielectric constant when compared to that of pure PVDF-TrFE at 10 kHz. Meanwhile, the dielectric constant of the composite shows improved thermal stability under a wide range of temperatures, from 30 °C to 150 °C, due to the 2D MTM and good compatibility between the HPANi-MTM and PVDF-TrFE matrix.

The scheme in Figure 1a shows the comparison between PVDF-TrFE and conductive HPANi doped PVDF-TrFE polymer (PVDF-TrFE/HPANi). HPANi has a high dispersion stability in PVDF-TrFE and leads to a percolative nanocomposite with an enhanced dielectric response. Optical images indicate the doping of HPANi turns the white PVDF-TrFE into dark green. The conductive fillers serve as active electrical sites for charge accumulation. The typical scanning electron microscopy (SEM) image in Figure 1b shows the cross-section view of a PVDF-TrFE/HPANi composite with an HPANi concentration of 1.0 wt%. The energy-dispersive X-ray spectroscopy (EDS, Figure S1) indicates the uniform distribution of HPANi in the PVDF-TrFE matrix through the nitrogen and fluorine elemental mapping, respectively. Figure 1c shows the dielectric constant of PVDF-TrFE/HPANi with various concentrations of HPANi under the frequency from 100 Hz to 10^6 Hz. Increasing the HPANi concentration results in a clear enhancement of the dielectric constant. The dielectric constant of PVDF-TrFE/HPANi composite at 10^3 Hz is plotted against the concentration of HPANi as shown in Figure 1d with a dramatic increase of dielectric constant from 8.9 to 243.6 upon the increase of HPANi concentration from 0.5 to 9.1 wt%. In contrast, there is a subtle change in the composite of PVDF-TrFE and nonconductive PANi, and the dielectric constant is 8.5 and 9.9 at the concentration of 9.1 and 16.7 wt%, respectively (Inset of Figure 1d and Figure S2). The concentration dependence of the dielectric constant is then fitted by the percolation theory following the equation $\varepsilon'=\varepsilon_m(f_c-f)^{-s}$, $f<f_c$, where ε' is the dielectric constant of PVDF-TrFE/HPANi composite sheet, ε_m is the dielectric constant of PVDF-TrFE, f_c is the percolation threshold, f is the filler concentration in the composite and s is the critical exponent in the insulating region.[25,26] The fitted line yields $f_c = 1.02$ and $s = 47.2$, in which the f_c value has a number higher than 1 indicating that the continuous increase of HPANi can enhance the dielectric constant. The PVDF-TrFE/HPANi composite sheets with an HPANi concentration of 50 wt% and pure conductive HPANi have a dielectric constant of 1005.7 and 1383.3, respectively (Figure S3). However, higher concentration of conductive HPANi introduces a larger dielectric loss with a higher dissipation factor. For example, the pure PVDF-TrFE has a dissipation factor of 0.03, which is increased to 0.04 in the PVDF-TrFE/HPANi composite after doping of 1.0 wt% of conductive HPANi (Figure S4). However, the dissipation factor can be greatly increased to 0.13 and 0.53 when the concentration of HPANi reaches to 4.8 wt% and 9.1 wt%, respectively. The application in dielectrics demands high dielectric constant and low dissipation factor.[27,28] However, aggregated fillers accompanied with increased defects in the composite sheet would dramatically increase the dielectric loss.[25] Regarding this, a uniform dispersion of conductive HPANi in the PVDF-TrFE matrix would be desirable. Therefore, we further utilize the solution process from the in-situ synthesized HPANi (s-HPANi) suspension to grow an all organic dielectric composite. The doping level of 1 wt% in concentration is selected by considering the dielectric constant and dissipation factor (< 0.1) for the following experiments.

A critical percolation concentration would be of great importance to exploit the conductor-insulator dielectric composite based on the percolation theory, which provides highly uniform dispersion and good compatibility between the additive and matrix phases. Therefore, an in-situ solution synthetic approach is adopted to grow PVDF-TrFE/s-HPANi composite by using in-situ s-HPANi network solution. In contrast with the PVDF-TrFE/HPANi composite with an opaque feature, the PVDF-TrFE/s-HPANi composite by in-situ solution growth is translucent. The as-synthesized s-HPANi is directly protonic doped with a fiber morphology as shown in the TEM image in Figure 2a and S5. The fabricated composite has a more uniform morphology as shown by the cross-section SEM image in Figure 2b. By comparing the dielectric constant of two different composite samples with the same HPANi concentration of 1.0 wt%, the PVDF-TrFE/s-HPANi composite through the in-situ solution process has a higher dielectric constant at the frequency range from 100 Hz to 10^6 Hz (Figure 2c) than that of PVDF-TrFE/HPANi and pure PVDF-TrFE. At the frequency of 10^3 Hz, the PVDF-TrFE/s-HPANi composite has a dielectric constant of 11.3, which is higher than that of PVDF-TrFE/HPANi and pure PVDF-TrFE with a dielectric constant of 10.8 and 8.4, respectively, while they have comparable dissipation factors between the two composite dielectric sheets (Figure S6). The temperature dependence of the dielectric behavior of PVDF-TrFE/s-HPANi composite is shown in Figure 2d. The dielectric constant reaches its maximum at 120 °C due to the ferroelectric transition in PVDF-TrFE matrix.

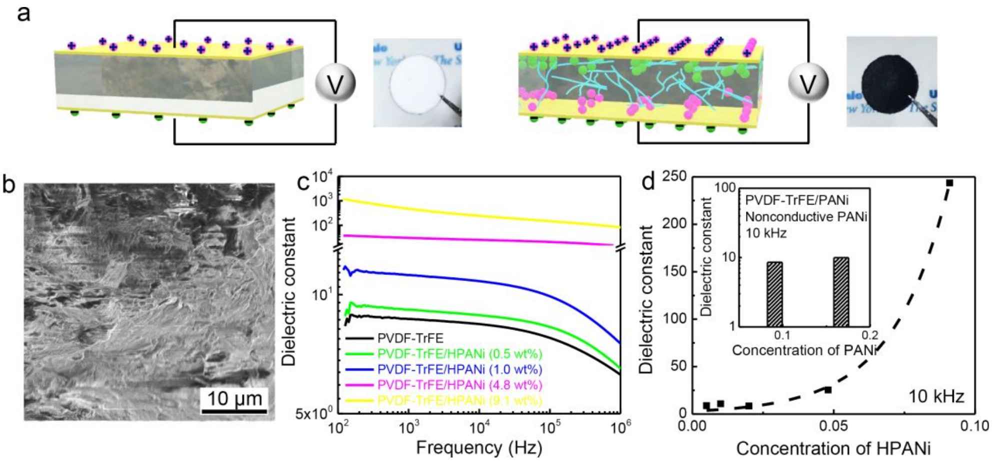

Figure 1. a) Scheme of PVDF-TrFE (left) and PVDF-TrFE doped with HPANi with a concentration of 1.0 wt% (right) and the corresponding optical images. b) SEM image of PVDF-TrFE doped with conductive HPANi containing 1.0 wt% of HPANi. c) Dielectric constant of PVDF-TrFE doped with different concentrations of conductive HPANi at various frequencies from 100 to 10^6 Hz. d) Dielectric constant of PVDF-TrFE doped with different concentrations of conductive HPANi at 10 kHz and fitting curve based on percolation theory. Inset is the dielectric constant of PVDF-TrFE doped with nonconductive HPANi with a concentration of 9.1 and 16.7 wt%.

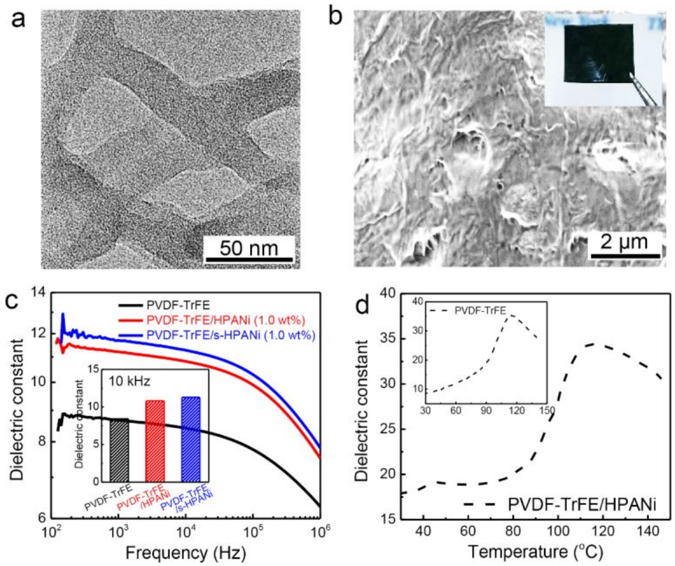

Figure 2. a) SEM image of PVDF-TrFE doped with synthesized conductive HPANi through solution process which indicates uniform dispersion. b) TEM image of synthesized conductive HPANi. c) Comparison of dielectric constant of PVDF-TrFE doped with commercial HPANi through solid process (Red, PVDF-TrFE/HPANi) and in-situ synthesized HPANi through solution process (Blue, PVDF-TrFE/s-HPANi). d) Dielectric constant of PVDF-TrFE doped with conductive HPANi at various temperatures from 30 to 150 °C. Inset is the dielectric constant of PVDF-TrFE at various temperatures from 30 to 150 °C.

To improve the thermal stability and the operating temperature of the dielectric composite, 2D montmorillonite (MTM) nanosheets through liquid exfoliation are introduced into the composite polymer.[30,31] As shown in Figure 3a, s-HPANi is in-situ polymerized onto the solution exfoliated 2D MTM nanosheets to obtain s-HPANi-MTM heterostructures followed by dispersion into the PVDF-TrFE matrix with a curing treatment. The successful synthesis of s-HPANi-MTM heterostructures is evidenced by the morphology characterization and XRD analysis (Figure 3b, 3c and S7). The s-HPANi-MTM heterostructures can be resolved in the TEM image in Figure 3b, showing the 2D layered polymeric structure. The typical SEM image and corresponding EDS mapping images indicates the dispersion of 2D MTM in s-HPANi polymer (Figure 3c and S8). The composite containing the s-HPANi-MTM heterostructures in the PVDF-TrFE matrix (PVDF-TrFE/s-HPANi-MTM) is fabricated to study its thermal stability. The differential scanning calorimetry (DSC) analysis is conducted on the PVDF-TrFE, PVDF-TrFE/s-HPANi, and PVDF-TrFE/s-HPANi-MTM composite from 25 °C to 140 °C as shown in Figure 3d. The PVDF-TrFE sheet has an exothermic peak at 92.0 °C corresponding to the crystallinity temperature, which is increased to 96.0 °C after doping with 1 wt% of HPANi.[32,33] In contrast, the PVDF-TrFE/s-HPANi-MTM composite shows an enhanced crystallinity temperature at around 111.4 °C due to the enhanced thermal stability of 2D MTM nanosheets. This increased transition temperature can also be found in s-HPANi-MTM heterostructures comparing with s-HPANi (Figure S9). The s-HPANi-MTM heterostructure can also improve the dielectric constant than that doped by s-HPANi and MTM, while higher doping concentration brings a higher dielectric constant. As shown in Figure 3e, the PVDF-TrFE/s-HPANi-MTM composite with 1 wt% of s-HPANi-MTM heterostrucutre has a higher dielectric constant through the frequency from 100 Hz to 10^6 Hz than those separately doped with 1 wt% of s-HPANi and MTM. The temperature dependent dielectric constant in Figure 3f shows that the PVDF-TrFE/s-HPANi-MTM composite has a lower variation under the temperature from 30 °C to 140 °C than that of PVDF-TrFE/s-HPANi, indicating the enhanced thermal stability of PVDF-TrFE/s-HPANi-MTM composite due to the incorporation of thermal conductive 2D MTM nanosheets. The peak in the dielectric constant is shifted to a higher temperature (125 °C) in PVDF-TrFE/s-HPANi-MTM composite due to the interaction between the PVDF-TrFE matrix with the thermal conductive 2D MTM nanosheets. The increased transition temperature results in a higher operation temperature compared with PVDF-TrFE and PVDF-TrFE/s-HPANi. Moreover, this composite sheet can be manufactured through direct writing with high flexibility, showing great promise in additive manufacturing of flexible dielectrics (Figure S10). As shown in Figure 3g, the printed PVDF-TrFE/s-HPANi-MTM sheets show a reliable dielectric constant through the frequency from 100 Hz to 10^6 Hz under intensive bending cycles of 90 degrees.

Conclusions

In conclusion, high dielectric performance of all polymer dielectrics is achieved by HPANi network and PVDF-TrFE bulk heterojunction, designed and guided by the percolation theory. To maintain a stable dielectric performance under the elevated temperature, liquid exfoliated thermal conductive 2D MTM nanosheets are utilized by in-situ hybridizing with HPANi to form PVDF-TrFE/s-HPANi-MTM composite, showing an improved thermal stability with low variation of dielectric constant and broader operation temperature window. More importantly, dielectric polymer composite can be manufactured by direct writing with high dielectric constant and flexibility, which opens up new avenues in the manufacturing of flexible hybrid electronics and radio frequency devices.

Acknowledgements

Financial support was provided by the U.S. Army Research Laboratory supports S. R. under Award W911NF-20-2-0016.

Conflicts of interest

There are no conflicts to declare.

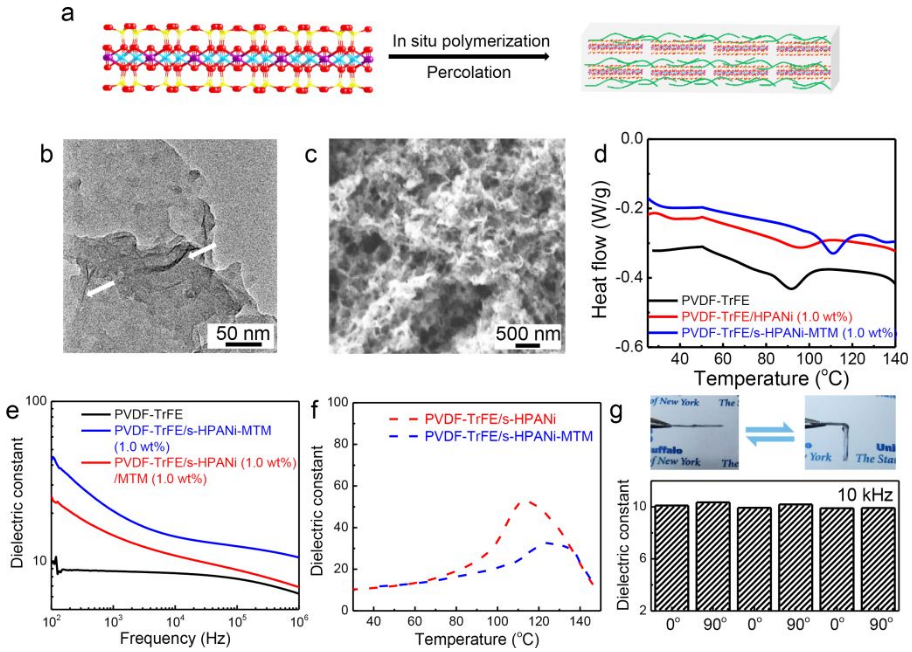

Figure 3. a) Illustrative scheme showing in situ polymerization of HPANi on 2D MTM and the fabrication of PVDF-TrFE/s-HPANi-MTM dielectric composite. b) TEM and c) SEM images of s-HPANi-MTM heterostructures. d) DSC curves of PVDF-TrFE, PVDF-TrFE/s-HPANi, and PVDF-TrFE/s-HPANi-MTM. e) Frequency dependent dielectric constant of PVDF-TrFE, PVDF-TrFE/s-HPANi-MTM, and PVDF-TrFE doped with s-HPANi and MTM separately. f) Temperature dependent dielectric constant of PVDF-TrFE/s-HPANi and PVDF-TrFE/s-HPANi-MTM with doping concentration of 1 wt%. g) Optical images of 3D printed PVDF-TrFE/s-HPANi-MTM under original and bending condition and the corresponding dielectric constant at the frequency of 10 kHz by bending and reverting for three times.

Notes and references

1 Prateek, V. K. Thakur, R. K. Gupta, *Chem. Rev.*, 2016, **116**, 4260–4317.

2 Q. Li, F. Z. Yao, Y. Liu, G. Zhang, H. Wang, Q. Wang, *Annu. Rev. Mater. Res.* 2018, **48**, 219–243.

3 Z. Yao, Z. Song, H. Hao, Z. Yu, M. Cao, S. Zhang, M. T. Lanagan, H. Liu, *Adv. Mater.*, 2017, **29**, 1601727.

4 J. Wang, X. Pang, M. Akinc and Z. Lin, *J. Mater. Chem.*, 2010, **20**, 5945–5949.

5 B. Jiang, J. Iocozzia, L. Zhao, H. Zhang, Y. Harn, Y. Chen and Z. Lin, *Chem. Soc. Rev.*, 2019, **48**, 1194–1228.

6 Q. Li, L. Chen, M. R. Gadinski, S. Zhang, G. Zhang, U. Li, E. Iagodkine, A. Haque, L. Q. Chen, N. Jackson, Q. Wang, *Nature*, 2015, **523**, 576–579.

7 L. Gao, J. He, J. Hu, Y. Li, *J. Phys. Chem. C*, 2014, **118**, 831-838.

8 W. Li, Q. Meng, Y. Zheng, Z. Zhang, W. Xia, Z. Xu, *Appl. Phys. Lett.*, 2010, **96**, 192905.

9 L. Zhu, Q. Wang, *Macromolecules*, 2012, **45**, 2937-2954.

10 D. Wilkinson, J. S. Langer, P. N. Sen, *Phys. Rev. B*, 1983, **28**, 1081–1087.

11 Z. M. Dang, Y. H. Lin, C. W. Nan, *Adv. Mater.*, 2003, **15**, 1625–1629.

12 L. Qi, B. I. Lee, S. Chen, W. D. Samuels, G. J. Exarhos, *Adv. Mater.*, 2005, **17**, 1777–1781.

13 Y. Shen, Y. Lin, M. Li, C. W. Nan, *Adv. Mater.*, 2007, **19**, 1418–1422.

14 L. A. Fredin, Z. Li, M. A. Ratner, M. T. Lanagan, T. J. Marks, *Adv. Mater.*, 2012, **24**, 5946–5953.

15 Y. Song, Y. Shen, H. Liu, Y. Lin, M. Li, C. W. Nan, *J. Mater. Chem.*, 2012, **22**, 16491.

16 X. Pang, Y. He, B. Jiang, J. Iocozzia, L. Zhao, H. Guo, J. Liu, M. Akinc, N. Bowler, X. Tan and Z. Lin, *Nanoscale*, 2013, **5**, 8695–8702

17 B. Jiang, X. Pang, B. Li and Z. Lin, *J. Am. Chem. Soc.* 2015, **137**, 11760–11767.

18 R. W. Johnson, J. L. Evans, P. Jacobsen, J. R. R. Thompson, M. Christopher, *IEEE Trans. Electron. Packag. Manuf.*, 2004, **27**, 164–176.

19 F. He, S. Lau, H. L. Chan, J. Fan, *Adv. Mater.*, 2009, **21**, 710–715.

20 S. Zhang, N. Zhang, C. Huang, K. Ren, Q. M. Zhang, *Adv. Mater.*, 2005, **17**, 1897–1901.

21 Z. M. Dang, L. Wang, Y. Yin, Q. Zhang, Q. Q. Lei, *Adv. Mater.*, 2007, 19, 852–857.

22 C. H. Ho, C. D. Liu, C. H. Hsieh, K. H. Hsieh, S. N. Lee, *Synth. Met.*, 2008, **158**, 630–637.

23 J. Li, P. Khanchaitit, K. Han, Q. Wang, *Chem. Mater.*, 2010, **22**, 5350–5357.

24 Y. Lu, J. Claude, B. Neese, Q. Zhang, Q. Wang, *J. Am. Chem. Soc.*, 2006, **128**, 8120–8121.

25 N. Maity, A. Mandal, A. K. Nandi, *J. Mater. Chem. C*, 2017, **5**, 12121–12133.

26 J. Y. Kim, T. Kim, J. W. Suk, H. Chou, J. H. Jang, J. H. Lee, I. N. Kholmanov, D. Akinwande, R. S. Ruoff, *Small*, 2014, **10**, 3405–3411.

27 X. Zhang, Y. Ma, C. Zhao, W. Yang, *Appl. Surf. Sci.*, 2014, **305**, 531–538.

28 J. Fu, Y. Hou, M. Zheng, Q. Wei, M. Zhu, H. Yan, *ACS Appl. Mater. Interfaces*, 2015, **7**, 24480–24491.

29 J. P. Calame, *J. Appl. Phys.*, 2006, **99**, 084101.

30 Y. Y. Zhang, S. L. Jiang, Y. Yu, G. Xiong, Q. F. Zhang, G. Z. Guang, *J. Appl. Polym. Sci.*, 2012, **123**, 2595–2600.

31 J. Zhu, X. Liu, M. L. Geier, J. J. McMorrow, D. Jariwala, M. E. Beck, W. Huang, T. J. Marks, M. C. Hersam, *Adv. Mater.*, 2016, **28**, 63–68.

32 J. Li, S. Tan, S. Ding, H. Li, L. Yang, Z. Zhang, *J. Mater. Chem.*, 2012, **22**, 23468.

Y. Liu, H. Aziguli, B. Zhang, W. Xu, W. Lu, J. Bernholc, Q. Wang, *Nature*, 2018, **562**, 96–100.

Table of contents

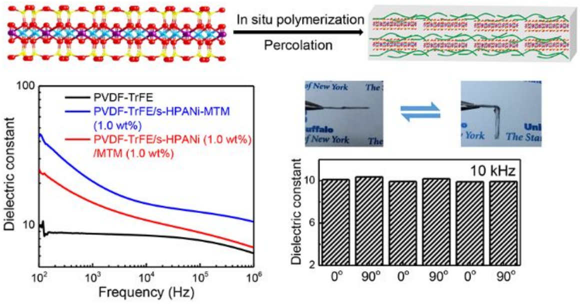

A printable dielectric polymer composite with enhanced dielectric constant and thermal stability.